

Giant nonlinear response of terahertz nanoresonators on VO₂ thin film

Jisoo Kyoung¹, Minah Seo¹, Hyeongryeol Park¹, Sukmo Koo², Hyun-sun Kim¹, Youngmi Park¹, Bong-Jun Kim³, Kwangjun Ahn¹, Namkyoo Park², Hyun-Tak Kim³, and Dai-Sik Kim^{1,*}

¹Center for Subwavelength Optics and Department of Physics and Astronomy,
Seoul National University, Seoul 151-747, Korea

²Photonic Systems Laboratory, School of EECS, Seoul National University, Seoul 151-744, Korea

³Metal-Insulator Transition Lab., ETRI, Daejeon 305-350, Korea

*dsk@phy.snu.ac.kr

Abstract: We report on an order of magnitude enhanced nonlinear response of vanadium dioxide thin film patterned with nanoresonators – nano slot antennas fabricated on the gold film. Transmission of terahertz radiation, little affected by an optical pumping for the case of bulk thin film, can now be completely switched-off: $\Delta T/T \approx -0.9999$ by the same optical pumping power. This unprecedentedly large optical pump-terahertz probe nonlinearity originates from the insulator-to-metal phase transition drastically reducing the antenna cross sections of the nanoresonators. Our scheme enables nanoscale-thin film technology to be used for all-optical switching of long wavelength light.

©2010 Optical Society of America

OCIS codes: (190.0190) Nonlinear optics; (050.1220) Apertures; (260.5740) Resonance

References and links

1. K. Jacobs, and A. J. Landahl, "Engineering giant nonlinearities in quantum nanosystems," *Phys. Rev. Lett.* **103**(6), 067201 (2009).
2. X. Hu, P. Jiang, C. Ding, H. Yang, and Q. Gong, "Picosecond and low-power all-optical switching based on an organic photonic-bandgap microcavity," *Nat. Photonics* **2**(3), 185–189 (2008).
3. R. Lopez, R. F. Haglund, L. C. Feldman, L. A. Boatner, and T. E. Haynes, "J. Richard F. Haglund, L. C. Feldman, L. A. Boatner, and T. E. Haynes, "Optical nonlinearities in VO[sub 2] nanoparticles and thin films," *Appl. Phys. Lett.* **85**(22), 5191–5193 (2004).
4. K. F. MacDonald, V. A. Fedotov, and N. I. Zheludev, "Optical nonlinearity resulting from a light-induced structural transition in gallium nanoparticles," *Appl. Phys. Lett.* **82**(7), 1087–1089 (2003).
5. N. I. Zheludev, "Nonlinear optics on the nanoscale," *Contemp. Phys.* **43**(5), 365–377 (2002).
6. M. Born, and E. Wolf, *Principles of Optics* (Cambridge University Press, Cambridge UK, 1999).
7. D. G. Cooke, F. A. Hegmann, E. C. Young, and T. Tiedje, "Electron mobility in dilute GaAs bismide and nitride alloys measured by time-resolved terahertz spectroscopy," *Appl. Phys. Lett.* **89**(12), 122103 (2006).
8. A. Leitenstorfer, S. Hunsche, J. Shah, M. C. Nuss, and W. H. Knox, "Femtosecond Charge Transport in Polar Semiconductors," *Phys. Rev. Lett.* **82**(25), 5140–5143 (1999).
9. S. Lysenko, A. J. Rua, V. Vikhnin, J. Jimenez, F. Fernandez, and H. Liu, "Light-induced ultrafast phase transitions in VO₂ thin film," *Appl. Surf. Sci.* **252**(15), 5512–5515 (2006).
10. G. L. Fischer, R. W. Boyd, R. J. Gehr, S. A. Jenekhe, J. A. Osaheni, J. E. Sipe, and L. A. Weller-Brophy, "Enhanced nonlinear optical response of composite materials," *Phys. Rev. Lett.* **74**(10), 1871–1874 (1995).
11. N. N. Lepeshkin, A. Schweinsberg, G. Piredda, R. S. Bennink, and R. W. Boyd, "Enhanced nonlinear optical response of one-dimensional metal-dielectric photonic crystals," *Phys. Rev. Lett.* **93**(12), 123902 (2004).
12. R. L. Nelson, and R. W. Boyd, "Enhanced electro-optic response of layered composite materials," *Appl. Phys. Lett.* **74**(17), 2417–2419 (1999).
13. J. H. Kang, J.-H. Choe, D. S. Kim, and Q. H. Park, "Substrate effect on aperture resonances in a thin metal film," *Opt. Express* **17**(18), 15652–15658 (2009).
14. E. Hendry, M. J. Lockyear, J. G. Rivas, L. Kuipers, and M. Bonn, "Ultrafast optical switching of the THz transmission through metallic subwavelength hole arrays," *Phys. Rev. B* **75**(23), 235305 (2007).
15. H.-T. Chen, W. J. Padilla, J. M. O. Zide, S. R. Bank, A. C. Gossard, A. J. Taylor, and R. D. Averitt, "Ultrafast optical switching of terahertz metamaterials fabricated on ErAs/GaAs nanoisland superlattices," *Opt. Lett.* **32**(12), 1620–1622 (2007).
16. W. J. Padilla, A. J. Taylor, C. Highstrete, M. Lee, and R. D. Averitt, "Dynamical electric and magnetic metamaterial response at terahertz frequencies," *Phys. Rev. Lett.* **96**(10), 107401 (2006).

17. W. L. Chan, H.-T. Chen, A. J. Taylor, I. Brener, M. J. Cich, and D. M. Mittleman, "A spatial light modulator for terahertz beams," *Appl. Phys. Lett.* **94**(21), 213511 (2009).
18. I. H. Libon, S. Baumgartner, M. Hempel, N. E. Hecker, J. Feldmann, M. Koch, and P. Dawson, "An optically controllable terahertz filter," *Appl. Phys. Lett.* **76**(20), 2821–2823 (2000).
19. W. L. Chan, M. L. Moravec, R. G. Baraniuk, and D. M. Mittleman, "Terahertz imaging with compressed sensing and phase retrieval," *Opt. Lett.* **33**(9), 974–976 (2008).
20. H. R. Park, Y. M. Park, H. S. Kim, J. S. Kyoung, M. A. Seo, D. J. Park, Y. H. Ahn, K. J. Ahn, and D. S. Kim, "Terahertz nanoresonators: Giant field enhancement and ultrabroadband performance," *Appl. Phys. Lett.* **96**(12), 121106 (2010).
21. F. J. Morin, "Oxides Which Show a Metal-to-Insulator Transition at the Neel Temperature," *Phys. Rev. Lett.* **3**(1), 34–36 (1959).
22. M. Nakajima, N. Takubo, Z. Hiroi, Y. Ueda, and T. Suemoto, "Photoinduced metallic state in VO₂ proved by the terahertz pump-probe spectroscopy," *Appl. Phys. Lett.* **92**(1), 011907 (2008).
23. D. J. Hilton, R. P. Prasankumar, S. Fourmaux, A. Cavalleri, D. Brassard, M. A. El Khakani, J. C. Kieffer, A. J. Taylor, and R. D. Averitt, "Enhanced photosusceptibility near T_c for the light-induced insulator-to-metal phase transition in vanadium dioxide," *Phys. Rev. Lett.* **99**(22), 226401 (2007).
24. P. U. Jepsen, B. M. Fischer, A. Thoman, H. Helm, J. Y. Suh, R. Lopez, and R. F. Haglund, "Metal-insulator phase transition in a VO₂ thin film observed with terahertz spectroscopy," *Phys. Rev. B* **74**(20), 205103 (2006).
25. A. Cavalleri, T. Dekorsy, H. H. W. Chong, J. C. Kieffer, and R. W. Schoenlein, "Evidence for a structurally-driven insulator-to-metal transition in VO₂: A view from the ultrafast timescale," *Phys. Rev. B* **70**, 161102–(2004).
26. A. Cavalleri, C. Tóth, C. W. Siders, J. A. Squier, F. Ráksi, P. Forget, and J. C. Kieffer, "Femtosecond Structural Dynamics in VO₂ during an Ultrafast Solid-Solid Phase Transition," *Phys. Rev. Lett.* **87**(23), 237401 (2001).
27. H.-T. Kim, B.-G. Chae, D.-H. Youn, S.-L. Maeng, G. Kim, K.-Y. Kang, and Y.-S. Lim, "Mechanism and observation of Mott transition in VO₂-based two- and three-terminal devices," *N. J. Phys.* **6**, 52 (2004).
28. Y. Shin, J. Moon, H. Ju, and C. Park, "Growth and electrical properties of vanadium-dioxide thin films fabricated by magnetron sputtering," *J. Korean Phys. Soc.* **52**(6), 1828–1831 (2008).
29. S. J. Yun, J. W. Lim, B.-G. Chae, B. J. Kim, and H.-T. Kim, "Characteristics of vanadium dioxide films deposited by RF-magnetron sputter deposition technique using V-metal target," *Physica B* **403**, 1381–1383 (2008).
30. B. G. Chae, H. T. Kim, and S. J. Yun, "Characteristics of W- and Ti-Doped VO₂ Thin Films Prepared by Sol-Gel Method," *Electrochem. Solid State* **11**(6), D53–D55 (2008).
31. P. A. George, J. Strait, J. Dawlaty, S. Shivaraman, M. Chandrashekar, F. Rana, and M. G. Spencer, "Ultrafast optical-pump terahertz-probe spectroscopy of the carrier relaxation and recombination dynamics in epitaxial graphene," *Nano Lett.* **8**(12), 4248–4251 (2008).
32. R. Huber, F. Tauser, A. Brodschelm, M. Bichler, G. Abstreiter, and A. Leitnerstorfer, "How many-particle interactions develop after ultrafast excitation of an electron-hole plasma," *Nature* **414**(6861), 286–289 (2001).
33. G. Segsneider, F. Jacob, T. Löffler, H. G. Roskos, S. Tautz, P. Kiesel, and G. Döhler, "Free-carrier dynamics in low-temperature-grown GaAs at high excitation densities investigated by time-domain terahertz spectroscopy," *Phys. Rev. B* **65**(12), 125205 (2002).
34. D. Grischkowsky, S. Keiding, M. Vanexter, and C. Fattinger, "Far-Infrared Time-Domain Spectroscopy with Terahertz Beams of Dielectrics and Semiconductors," *J. Opt. Soc. Am. B* **7**(10), 2006–2015 (1990).
35. Z. Jiang, M. Li, and X. C. Zhang, "Dielectric constant measurement of thin films by differential time-domain spectroscopy," *Appl. Phys. Lett.* **76**(22), 3221–3223 (2000).
36. J. Lee, M. Seo, D. Park, D. Kim, S. Jeoung, Ch. Lienau, Q. H. Park, and P. Planken, "Shape resonance omnidirectional terahertz filters with near-unity transmittance," *Opt. Express* **14**(3), 1253–1259 (2006).
37. G. Gallot, and D. Grischkowsky, "Electro-optic detection of terahertz radiation," *J. Opt. Soc. Am. B* **16**(8), 1204–1212 (1999).
38. M. A. Seo, H. R. Park, S. M. Koo, D. J. Park, J. H. Kang, O. K. Suwal, S. S. Choi, P. C. M. Planken, G. S. Park, N. K. Park, Q. H. Park, and D. S. Kim, "Terahertz field enhancement by a metallic nano slit operating beyond the skin-depth limit," *Nat. Photonics* **3**(3), 152–156 (2009).
39. M. Seo, J. Kyoung, H. Park, S. Koo, H. S. Kim, H. Bernien, B. J. Kim, J. H. Choe, Y. H. Ahn, H.-T. Kim, N. Park, Q. H. Park, K. Ahn, and D. S. Kim, "Active terahertz nanoantennas based on VO₂ phase transition," *Nano Lett.* **10**(6), 2064–2068 (2010).
40. J. W. Lee, M. A. Seo, D. J. Park, S. C. Jeoung, Q. H. Park, Ch. Lienau, and D. S. Kim, "Terahertz transparency at Fabry-Perot resonances of periodic slit arrays in a metal plate: experiment and theory," *Opt. Express* **14**(26), 12637–12643 (2006).
41. J. W. Lee, M. A. Seo, J. Y. Sohn, Y. H. Ahn, D. S. Kim, S. C. Jeoung, Ch. Lienau, and Q. H. Park, "Invisible plasmonic meta-materials through impedance matching to vacuum," *Opt. Express* **13**(26), 10681–10687 (2005).
42. D. J. Park, S. B. Choi, Y. H. Ahn, F. Rotermund, I. B. Sohn, C. Kang, M. S. Jeong, and D. S. Kim, "Terahertz near-field enhancement in narrow rectangular apertures on metal film," *Opt. Express* **17**(15), 12493–12501 (2009).
43. M. A. Seo, A. J. L. Adam, J. H. Kang, J. W. Lee, K. J. Ahn, Q. H. Park, P. C. M. Planken, and D. S. Kim, "Near field imaging of terahertz focusing onto rectangular apertures," *Opt. Express* **16**(25), 20484–20489 (2008).
44. F. J. García-Vidal, E. Moreno, J. A. Porto, and L. Martín-Moreno, "Transmission of light through a single rectangular hole," *Phys. Rev. Lett.* **95**(10), 103901 (2005).

45. J. W. Lee, M. A. Seo, D. H. Kang, K. S. Khim, S. C. Jeoung, and D. S. Kim, "Terahertz electromagnetic wave transmission through random arrays of single rectangular holes and slits in thin metallic sheets," *Phys. Rev. Lett.* **99**(13), 137401 (2007).
46. D. J. Park, S. B. Choi, Y. H. Ahn, Q. H. Park, and D. S. Kim, "Theoretical Study of Terahertz Near-Field Enhancement Assisted by Shape Resonance in Rectangular Hole Arrays in Metal Films," *J. Korean Phys. Soc.* **54**(1), 64–70 (2009).
47. N. Laman, and D. Grischkowsky, "Terahertz conductivity of thin metal films," *Appl. Phys. Lett.* **93**(5), 051105 (2008).
48. T. I. Jeon, J. H. Son, K. H. An, Y. H. Lee, and Y. S. Lee, "Terahertz absorption and dispersion of fluorine-doped single-walled carbon nanotube," *J. Appl. Phys.* **98**(3), 034316 (2005).
49. A. Taflove, and S. C. Hagness, *Computational Electromagnetics: The Finite-Difference Time-Domain Method* (Artech House, Boston, 2000).

1. Introduction

Nonlinearities in optics have been of considerable interest for both science and engineering, for instance in quantum-to-classical transition and in all-optical switching or optical computing [1,2]. In most nonlinear materials, the complex index of refraction can be written as $\hat{n} = n + i\alpha/2k_0$ ($k_0 =$ vacuum wave vector) where n and α are, respectively, the real part of the refractive index and the absorption coefficient, both of which experience pump-induced nonlinear changes [3–5]. Thin layers of semiconductors and strongly correlated electron systems have been powerful candidates for all-optical switching devices at long wavelength regime, due to their excellent optical properties such as fast carrier dynamics and pump-induced large nonlinearity.

For the thin film, however, despite the large nonlinearity, corresponding nonlinear response $\Delta T/T$ (the ratio between the differential transmission and the transmission through the film) is too small, limiting potential photonic applications because nearly constructive multiple interference in the thin film tends to push the transmittance towards unity [6] even when the thin film dielectric constants are large. In other words, the product of the pump-induced change of the absorption coefficient $\Delta\alpha$ and the film thickness or nonlinear interaction length L is much less than one [4,5]. For example, the optical constants of a few μm -thick semiconductor thin films are dramatically changed at terahertz range by optical pumping, but the corresponding transmission or reflection change is just a few percents [7–9]. Consequently, to have a huge transmission change, all the way to the complete extinction case of $\Delta T/T \approx 1$ induced by optical pumping, one should force the *effective* nonlinear response $\Delta\alpha L$ to be close to one.

In this regards, many attempts were made to overcome the small nonlinear response of thin film. Forming a composite of one material with another, which has different optical characteristics compared with the previous one, is a common approach to induce enhanced nonlinearity in the visible and the near infrared regime [10–12]. For the longer wavelength regime, one effective way is to fabricate metamaterials on semiconductor substrates. Since the resonance wavelength and also transmission are strongly affected by the refractive index of the substrate [13], patterning of the rectangular hole arrays on a thin film can enhance performance of the devices at the shape resonance. In particular, a factor of 2~5 improvement, compared with bare film, in nonlinear response was achieved by fabricating metallic antenna structure arrays [14–16]. However, the perfect transmission control of the long wavelength light is essential to fully utilize the excellent optical properties of the thin film, for instance for Fourier optical, spatial and temporal pulse shaping or a terahertz filter [17–19]. In this work, we show that the absolute switching of terahertz electromagnetic wave with optical pump can be achieved by fabricating nanoresonators [20] whose width is in nanometer scale, on a vanadium dioxide (VO_2) thin film.

2. Experimental results and discussions

Vanadium dioxide (VO_2), a strongly-correlated compound, undergoes first-order insulator-to-metal phase transition at critical temperature $T_c = 340$ K [21,22]. This phase transition is reversible and during this transition, the crystal structure changes from monoclinic at low

temperature to rutile at high temperature [Fig. 1(a)]. The conductivity jumps by several orders of magnitude and optical constants experience large changes through this transition [23,24], which can also be induced optically or electrically [22,25–27]. Our 100-nm-thick VO₂ thin films were grown on 430- μ m-thick C-plane Al₂O₃ substrates by radio-frequency magnetron sputtering method whereas the sol-gel method is used to grow 25-nm-thick VO₂ thin films on the same substrate [28–30].

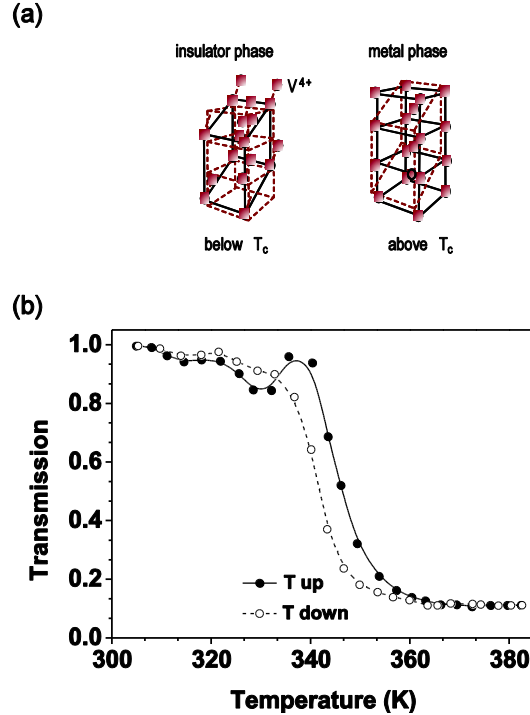


Fig. 1. (a) Schematic description of the two crystal structures of VO₂: the insulator (monoclinic) phase below the critical temperature $T_c = 340$ K and the metal (rutile) phase above T_c . Only vanadium atoms are visualized in the figure and each atom is surrounded by an oxygen octahedron. (b) The temperature-dependent hysteresis of the THz transmittance through an un-patterned 100-nm-thick VO₂ thin film at 0.4 THz (raising (lowering) temperature: filled (empty) circle). Hysteresis curve shows that the critical temperature T_c of our sample is about 345 K.

Terahertz time-domain spectroscopy (THz - TDS) is a powerful tool to detect the insulator-to-metal phase transition in VO₂ since THz wave is quite sensitive to the free carrier response [31–33]. Our THz - TDS system has a spectral range from 0.1 to 2.0 THz. The output of a 130 fs Ti:sapphire mode-locked laser (coherent Mira) and a semi-insulating GaAs emitter biased with 50 kHz and 150 V square voltage pulses are employed to generate a single-cycle THz pulse. Electro-optic detection method is chosen to measure the transmitted time-domain signals. After Fourier transforming time traces, we obtain transmitted amplitude and phase information [34–37]. We firstly measure the THz transmittance of our bare VO₂ thin films as a function of temperature [Fig. 1(b)]. We attach our sample on a reference aperture of 1 mm by 1 mm [38] and control the temperature using a heater. The temperature of the sample is monitored by reading the resistivity of thermistors (SEMITEC 104JT-015). Transmittance at $T = 310$ K is used as a reference. Figure 1 (b) shows a typical hysteresis curve of the normalized transmittance (filled (empty) circles for temperature up (down)) at a selected frequency, 0.4 THz, which exhibits the critical temperature T_c at 345 K. In metallic state, the complex index of refraction is deduced from the transmitted THz wave to be about $85 + 86i$ at 0.4 THz, in good agreement with earlier works [23,24].

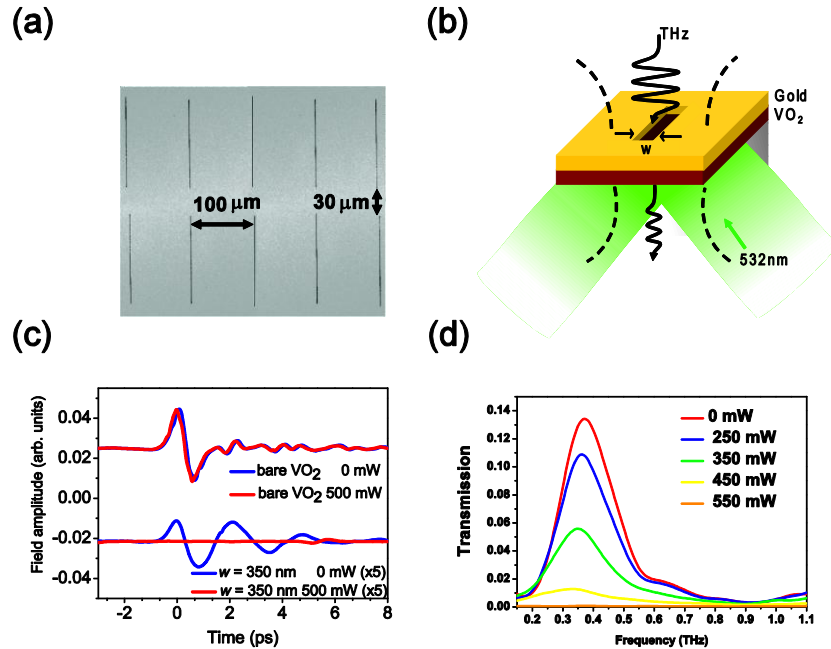


Fig. 2. (a) Scanning electron microscopy (SEM) image of our sample patterned with 350-nm-width resonators on 100-nm-thick VO₂ film using electron beam lithography. The thickness of the gold layer is 100 nm and the horizontal period of the rectangle hole array is 100 μm and the vertical 130 μm. (b) Schematic of our photo excitation experiments. Single cycle THz pulse impinges on the gold surface first and passes through the VO₂ side. The pump laser at 532 nm wavelength, illuminates the back side of the sample and induces phase transition of the VO₂ thin film. (c) Time traces for bare VO₂ (top) and nanoresonator patterned (bottom) samples with zero (blue lines) and 500 mW (red lines) absorbed pumping power. For the bare film, the difference between the signals with and without pumping is hardly recognizable while quasi-periodic feature, due to the fundamental half wavelength resonance, completely disappears with the same pumping power for the nanoresonator patterned sample. (d) Fast Fourier transform of the measured THz pulse for 350-nm-width rectangle hole array patterned sample exhibit strong resonance characteristic at the zero pumping power. The transmission at the resonance frequency is completely extinct when the pumping power reaches 550 mW.

To enhance the optical nonlinearity, we pattern the μm- and nm-width resonators, forming periodic array of slot antennas, using electron beam lithography [20] on a 100-nm-thick gold layer deposited on VO₂/Al₂O₃ [39]. Figure 2 (a) shows a scanning electron microscopy (SEM) image of our sample patterned with 350-nm-width nanoresonators. The length of each resonator is fixed at $L = 150 \mu\text{m}$. The horizontal period of the rectangle hole array is 100-μm and the vertical period 180-μm. The 27-μm-width sample has the same periodicities. In order to induce optical nonlinearity, we excite our samples using 2.33 eV continuous wave laser (532 nm wavelength) focused onto a 1.5 millimeter spot size covering the whole pattern area [Fig. 2(b)] and measure the THz transmission while raising the optical pumping power. The incident THz polarization is along the short side of the resonators.

Figure 2(c) compares time-domain transmission signals for the un-patterned (top) and the nano-patterned (bottom; $w = 350 \text{ nm}$) sample with (red line) and without (blue line) pump. For the un-patterned sample, the two terahertz pulses can be hardly distinguishable, indicating no significant transmission change up to 500 mW of *absorbed* pumping power. The absorbed power is deduced from the incident power subtracted with the reflected and transmitted power ($A = 1 - R - T$) for bare and patterned samples, respectively. In stark contrast to the bare film case, for the nano-patterned sample, the transmitted signal, which displays quasi-periodic feature due to the fundamental half wavelength resonance [40,41], completely disappears with the same pumping power. Transmission spectra shown in Fig. 2(d), obtained from fast Fourier

transforming time-domain signals with increasing pump power, display the strong resonant feature being turned-off until no transmission remains. Resonance frequency 0.375 THz is dictated by the antenna length and VO₂ index of refraction at the insulating phase [13,42–44]. Since the horizontal period of our rectangular hole arrays is subwavelength, the spectrum does not include any Rayleigh minima [45,46].

Displayed in Fig. 3(a) are differential transmissions at 0.375 THz for bare (filled gray triangle), $w = 27 \mu\text{m}$ (filled blue square) and $w = 350 \text{ nm}$ (filled red circle) patterned samples, as a function of the excitation power. While only 50% change in transmission is seen for the bare sample at the maximum pumping power, over 99.99% extinction is clearly visible for the $w = 350 \text{ nm}$ sample. Comparing the differential transmission of μm -size sample with that of nm-size one shows that nano-patterned case gives rise to much more drastic extinction with increasing photo-excitation power. Meanwhile, differential transmission as a function of pump power becomes more gradual as the slot width decreases.

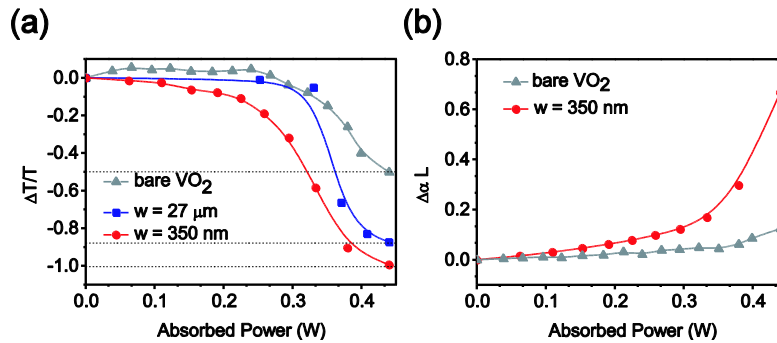


Fig. 3. (a) The differential transmission signals of a bare VO₂ film (filled gray triangle), 27 μm (filled blue square) and 350 nm (filled red circle) width antenna arrays on VO₂ films at the resonance frequency (0.375 THz) as a function of the pumping power. Only small changes in transmission are seen for the bare sample, while perfect extinction is clearly visible for the 350-nm-width resonators patterned sample above 450 mW of absorbed power. (b) Nonlinear response of the bare and nanoresonator patterned sample. Nonlinear response suddenly increases at some critical pumping power, 300 mW, as the VO₂ thin film undergoes insulator-to-metal phase transition.

Figure 3(b) shows the changes of *effective* nonlinear responses ($\Delta\alpha L$) at 0.375 THz due to optical pump for unpatterned (filled gray triangle) and nano-patterned (filled red circle) samples, respectively. The absorption coefficients of the bare film are estimated from the amplitude and phase information of the transmitted terahertz wave [34,47,48]. We use the same method with the patterned sample regarding the patterned gold layer together with VO₂ thin film as a homogeneous material. For the bare film, the nonlinear responses are always less than 0.2 explaining the small terahertz transmission modulation. However, the *effective* nonlinear response of the nano-patterned sample is hugely enhanced and exhibits quite different feature compared with the un-patterned case. Nonlinear response of the nano-patterned sample is always larger than that of the un-patterned one but it suddenly increases at some critical pumping power, 350 mW, indicating optical pump-induced insulator-to-metal phase transition, and finally reaches the value of 0.7.

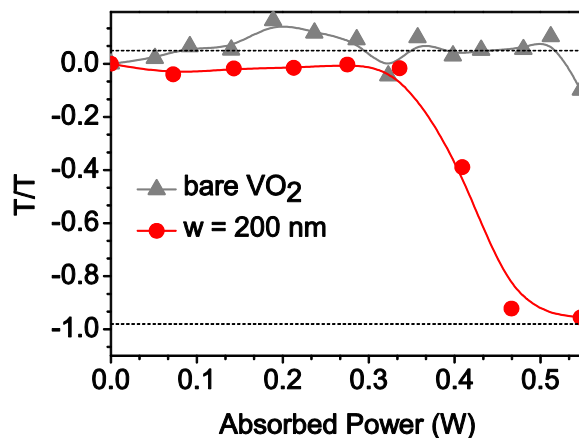


Fig. 4. The differential transmissions for the 25-nm-thick bare VO₂ film (filled gray triangle) and 200-nm-width slot antenna patterned sample (filled red circle) are measured at 0.42 THz. For the bare film, no changes are seen due to optical pumping while near perfect switching performance is observed with the patterned sample.

Further reducing the thickness of the VO₂ thin film from 100 nm to 25 nm gives even more dramatic results when comparing the patterned and un-patterned samples. Figure 4 shows the differential transmissions for the 25-nm-thick bare VO₂ film (filled gray triangle) and 200-nm-width slot antenna patterned sample (filled red circle), measured at 0.42 THz, respectively. We can hardly see any change due to optical pumping for the un-patterned sample while near perfect switching performance is observed with the patterned sample. Clearly, this result shows that our novel strategy, nano-size patterning, to enhance the optical nonlinear response, can also be applicable to the ultra thin film corresponding to $\sim\lambda/30,000$.

To better understand the physical origin of enhanced nonlinear response, we have carried out finite-difference time-domain (FDTD) method modeling using asymptotically varying grid sizes [49]. We use $\hat{n}=3$ for insulating state of VO₂ and $10.24+10.10i$ for metal state. The incident wave comes from the left side. Figure 5(a) and 5(b) show the time-averaged electric-field intensity for $\lambda = 34.48 \mu\text{m}$ in the presence of patterned VO₂ film without and with optical pumping, respectively. Simulation results explain how our nano-patterned sample can enhance the nonlinear response. A single nanoresonator located at the center has 100-nm-width and 10- μm -length with $\lambda = 34.48 \mu\text{m}$ as the fundamental resonance wavelength. Since the rectangular hole strongly attracts surrounding electromagnetic waves and funnels them (Fig. 5(a)), electric field inside the hole is hugely enhanced, and such field enhancement keeps increasing with decreasing rectangle width at the resonance [38,43,44]. Electrostatic energy stored in tiny volume of the narrow slots results in enhanced far-field transmission for the insulating VO₂ [38,42]. In stark contrast, when the underlying film becomes metallic, it effectively shuts off the resonator and eliminates funneling effect resulting colossal transmission extinction (Fig. 5(b)). These FDTD simulations well explain the role of nanoresonators for enhanced nonlinear response at least qualitatively

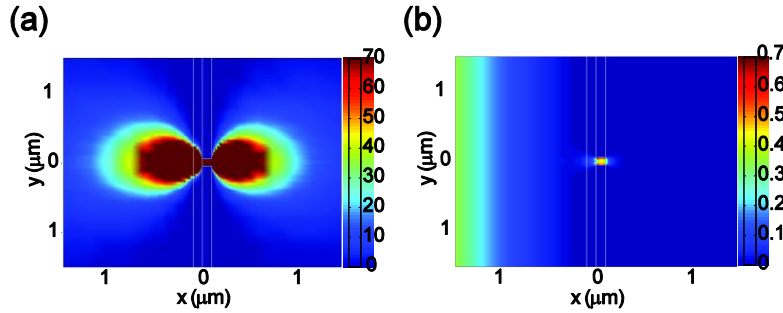


Fig. 5. Averaged horizontal electric field for $\lambda = 34.48 \mu\text{m}$ calculated by finite difference time domain (FDTD) method to investigate the physical origin of enhanced nonlinear response of nanoresonators. The incident wave comes from the left to the right. (a) patterned sample with insulating state of VO_2 (b) patterned sample with metal state of VO_2 . For the patterned film case, nanoresonators attract surrounding waves and funnel them to the other side making enhanced transmission at the insulating state of VO_2 while most of the beam reflects back at the surface when the VO_2 film is in the metallic state.

3. Conclusion

In conclusion, we have demonstrated that VO_2 thin film with nm-width rectangular apertures comprises a new class of metamaterial achieving orders of magnitudes improvement in extinction with modest photo-excitation power, overcoming multiple-interference in thin-films. Strongly localized near field in the resonators induces the enhanced far-field transmission for the insulating VO_2 while the resonators are completely inoperative when the underlying VO_2 film becomes fully metallic, making perfect transmission control possible. Corresponding giant enhanced nonlinear response $\Delta\alpha L$ reaches 0.7 with 350-nm-width patterned sample, despite ultrathin film thickness. Room temperature carrier lifetime of the order of picosecond for VO_2 [22,23] strongly suggests the potential use of nano-patterned VO_2 thin films for all-optical switching having huge dynamic range. Our new scheme bridges the gap between thin film technology, nanotechnology and active metamaterials research.

Acknowledgments

The authors gratefully acknowledge the assistance of Prof. R. Huber and Dr. R. Lopez for nice discussion and the SEMITEC, Innochips Technology and Tnest in offering excellent thermistors. This research was supported by the Korea Science and Engineering Foundation (KOSEF) (SRC, No:R11-2008-095-01000-0) and the Korea Research Foundation (KRF) grant funded by the Korea government (MEST) (No:2009-0071309), KICOS (GRL, K2081500003), Seoul Science Fellowship and the Seoul R&BD Program(10543).